Supplemental data

Phantom Preparation

Initially, our aim was to employ agar phantoms with stiffness comparable to blood clots (Young's modulus on the order of 2 kPa) (Carr *et al* 2002); however, we found that they were not sufficiently durable for multiple rounds of imaging. Accordingly, we chose a more stiff sample of 1% agar (nominally 18 kPa measured with a TA.XT Plus, Texture technologies) under the assumption that our results will, if anything, under-report the available magnetomotive contrast compared to that in less stiff blood clots, because motion amplitude is inversely proportional to elastic modulus. For SPIO concentration-dependent studies, homogenously suspended Fe_3O_4 nanoparticles (Sigma Aldrich, 637106-250G) were prepared according to a modified version of a previously established protocol (Acar *et al* 2005). For our purposes, we combined Fe_3O_4 nanoparticles, dodecanoic acid, and NH_3 at 30 mg/ml, 10 mg/ml, and 10% (v/v) concentrations, respectively, in distilled H_2O. This solution was sonicated for 5 intervals of 5 hours over the course of 3 days. The suspended particles were separated from unsuspended particles by decanting the suspension into a beaker while holding a permanent magnet near the base of the container. The final Fe concentration was measured by mass spectrometry to be 0.91 mg Fe/ml.

Phantoms simulating the mechanical and acoustic properties of tissue were made with and without SPIOs in 8 cm diameter, 8 cm deep cylindrical plastic molds according to a modified version of a previously published protocol (Madsen 1978). For SPIO concentration-dependent studies we prepared homogenous tissue phantoms starting from varying dilutions of the stock SPIO solution in water to achieve the desired concentrations (0×, 1×, 2×, 4×, 5×, and 10×). Accordingly, the phantom solution was created by melting agar powder (Acros Organics 40040) at 1% concentration in either SPIO stock solution (diluted with DI water to desired concentration) or water (for control) at 80^{o}C for 15 minutes. The solution was then allowed to cool to 65^{o}C at which point 0.0275 ml aqueous Kodak Photoflo 200/ml (to aid in suspension of graphite powder) was added, followed by graphite powder at 15 mg/ml. Once thoroughly mixed, the phantom solution was poured into the plastic molds and immediately covered and surrounded in an ice bath for rapid cooling. For the concentration dependent study we acquired data with the US transducer positioned at 3 different locations on the phantom surface.

For phantoms with clot-like SPIO inclusions, a 1 cm^3 Styrofoam cube was suspended 1 cm below the top of the phantom mold to create a void centered in the middle of the phantom. The control agar-graphite solution prepared as above was poured to a level that very nearly covered the Styrofoam cube. After the agar solidified, the cube was carefully removed and the void was filled with 1000 μl of either the SPIO solution or control solution with no SPIOs. 50 ml of control solution was then added to fill the remaining space in the phantom mold.

For the platelet rich clots, the agar phantoms were made as described above with the exception that the voids were made with 1 cm long, 0.25 in diameter cylinders. To form the clots by recalcification the concentrated platelet/CS solutions (having already gone through the incubation process) were transferred to 1.5 ml Eppendorf tubes and pelleted again to remove CS. The pellets were resuspended in 250 μl of PPP, followed by the addition of 8 mg graphite powder (to aide in acoustic scattering), and 100 μl of RBCs (for additional acoustic scattering). An additional 100 μl of platelet stock solution was added to enhance clotting. The solutions were mixed thoroughly. Finally, 15 μl of 1 molar $CaCl_2$ was stirred into each Eppendorf tube to induce clotting by recalcification. The clotting mixtures were allowed to sit for 30 minutes after which the clot was removed from the Eppendorf tube and transferred to an agar phantom with a 250 μl cylindrical void. The phantom was then capped with 50 ml of control agar solution to fill the remaining space.

Determination of Vibration Amplitude Sensitivity

To explore the vibration amplitude sensitivity of our system we analyzed the motion detected in the homogeneous tissue phantom at the lowest Fe concentration (0.091 mg Fe/ml) in the following way. First, we selected a 10 by 10 pixel region in an area of the phantom for which the nominal MMUS signal was 3 dB -- for this case the region was centered in the area of highest MMUS SNR (toward the edge of the phantom where the magnetic forces are strongest). Data within this region were collected with the field modulated and field off, and were processed in the same way. First, the differential phases for these pixels were spatially averaged and the amplitude of the corresponding FFT at 2 Hz was calculated. As seen in Supplemental Figure 1, the phase noise from the field modulated and field off data has a similar profile, while the FFT of the field modulated data has a peak at 2 Hz. To better illustrate the magnitude of the mechanical vibration required to cause a peak of this amplitude, we simulated the phase modulation induced by a magnetically-driven motion at 2 Hz with vibration amplitude of 3.7 nm.

(The phase modulation was computed using the relationship $\Delta z = \frac{\Delta\phi}{4\pi}\frac{c}{f}$, where c is the average speed of sound in tissue (1540 m/s), and f is the ultrasonic center frequency (10 MHz). The displacement amplitude of 3.7 nm is then equivalent to a phase modulation amplitude of 0.8 mrad. Note: This calculation assumes a constant center frequency, a more accurate displacement estimate would include a correction factor for the fact that the ultrasound center frequency changes with depth.)

The simulated 2 Hz sine wave was then added to the random differential phase of the field off data set, and the resulting Fourier spectrum is shown in the bottom row of Supplemental Figure 1. We see that this added phase modulation is capable of creating a Fourier peak comparable in height to that of the field-modulated data set. To further illustrate the vibration amplitude detection we show the inverse FFT after bandpassing the original FFTs at 2 Hz. From the iFFT the phase of the vibration becomes more clear—for the Field Modulated data and the simulated vibration data the phase of the motion is approximately 0 radians while the phase of the Field Off data is ~ 0.83 radians (random). The fact that the phase of the mechanical vibration is predictable only for the Field Modulated data illustrates the purpose of our phase filtering algorithm to provide increased noise rejection.

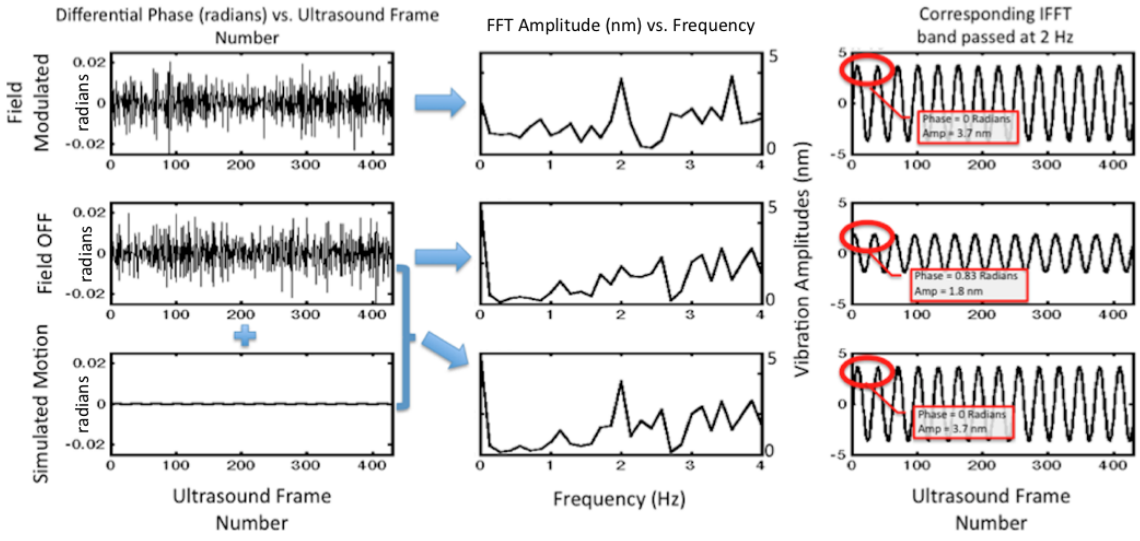

Supplemental Figure 1. Demonstration of vibration amplitude sensitivity analysis.

Supplemental References

Acar H Y, Garaas F S, Syud F, Bonitatebus P and Kulkarni A M 2005 Superparamagnetic nanoparticles stabilized by polymerized PEGylated coatings *J. Magn. Magn. Mater*. **293** 1–7

Carr M E, Krishnaswami A and Martin E 2002 Platelet contractile force (PCF) and clot elastic modulus (CEM) are elevated in diabetic patients with chest pain *Diabetic medicine: a journal of the British Diabetic Association* **19** 862–6

Madsen E 1978 Tissue mimicking materials for ultrasound phantoms *Med. Phys.* **5** 391